Kinetics of Thermally Induced Phase Separation in a Crystallizable Polymer Solution

ARTICLE *in* MACROMOLECULES · MARCH 1998

Impact Factor: 5.8 · DOI: 10.1021/ma971056p

2 AUTHORS, INCLUDING:

Anthony J. Mchugh
Lehigh University
166 PUBLICATIONS **3,443** CITATIONS

Dynamics of Spinodal Decomposition in Polymer Solutions near a Glass Transition

B. F. Barton, P. D. Graham, and A. J. McHugh*

Department of Chemical Engineering, University of Illinois, Urbana, Illinois 61801

Received July 1, 1997; Revised Manuscript Received December 26, 1997

ABSTRACT: A model based on the Cahn−Hilliard formalism is used to simulate structure formation in thermally quenched polymer solutions in the vicinity of a glass transition. Simulation results for the system poly(methyl methacrylate)/cyclohexanol are correlated with light scattering and microscopy measurements recently reported in the literature. Good qualitative and quantitative agreement with experimental observations indicates the applicability of current free-volume and thermodynamic theories to quantify the dynamics near a glass transition. The model accurately predicts late-stage scaling exponents, and results show that the early stage of phase separation occurs on time scales $\ll 1$ s. Pore growth rates based on zero-free-parameter calculations agree well with experimental observations. Simulations also show that quenching a phase-separated structure below a glass transition can result in the formation of a secondary droplet structure within the polymer-rich phase, prior to freezing-in of the preexisting morphology. Such secondary structures, which have also been observed experimentally, appear to have little or no effect on the calculated structure factor, which is also consistent with light-scattering measurements.

Introduction

Thermal-induced phase separation is a common technique for producing composite materials from polymeric blends and porous polymer membranes from solutions. In the latter case, the ability to predict and thereby control the morphology of the resulting film is critical in attaining desired material properties, such as membrane selectivity and mechanical integrity. The object is to lock in desired morphologies at some intermediate stage of the phase separation by solidification of one or both phases via gelation, crystallization, or a glass transition mechanism. Such an arrest of structure growth has been observed experimentally by light-scattering measurements for a gelatinous system[1] and, most recently, for a binary polymer solution.[2] From a computational perspective, it is therefore of great importance to model the dynamics of structure growth in the vicinity of such a transition.

For homogeneous solutions exhibiting an upper critical solution temperature (UCST), phase separation can be induced by a temperature quench below the binodal. Depending on the location in the two-phase region to which the solution is quenched, structure growth proceeds by either nucleation and growth (NG) or spinodal decomposition (SD). Nucleation and growth occurs in the metastable region of the phase diagram and takes place by concentration fluctuations that are large in magnitude but small in extent (i.e., by the formation of a nucleation site of sufficient size whose composition is that of the equilibrium binodal), as smaller fluctuations dissipate due to surface energy costs. Spinodal decomposition, on the other hand, takes place in the unstable region of the phase diagram by rapid initial growth of infinitesimal concentration fluctuations that are large in extent. These fluctuations reach their binodal compositions in the so-called late stage of the transformation. From mean-field considerations, the boundary between NG and SD is distinct and represented by the spinodal curve.[3] However, recent numerical[4] and experimental[5] evidence suggests that the transition between the two mechanisms is gradual and the two may, in certain instances, occur simultaneously.

Phase separation by spinodal decomposition is described by Cahn−Hilliard theory which expresses the free energy in a phase-separated system as a function of both composition and the spatial gradients in composition. As a result, there is a complex interplay between the homogeneous or bulk free energy component, which drives the two phases toward their equilibrium compositions, and the surface energy component, which attempts to minimize the interfacial area in the system. Modeling of phase separation in binary systems using Cahn−Hilliard theory, particularly for polymer blends, has been an intense area of research.[6−9] More recent work has also explored the mechanism of domain pinning in some polymer blends.[10,11] In addition, several recent studies have begun to elucidate the qualitative effects a glass transition or gelation might have on the phase separation dynamics predicted by Cahn−Hilliard theory. Sciortino et al.[12] studied a system undergoing simultaneous phase separation and gelation and showed that domain growth can be arrested once a sufficient gel concentration is established. Sappelt and Jackle[13,14] have studied the effect of a glass transition boundary in a binary liquid mixture and have shown that coarsening is not completely halted but rather the structure can continue to grow by a coalescence mechanism. However, this behavior has not been experimentally observed, and current observations[2] suggest the glass transition arrests structure formation on any realistic time scale. Despite the wealth of literature on phase separation in polymer blends and binary mixtures, little theoretical work has focused on polymer solutions[15,16] and, to our knowledge, no work yet has discussed quantitative prediction of structure growth kinetics in such systems.

In this study, the dynamics of phase separation in polymer solutions near a glass transition is modeled using a Cahn−Hilliard formalism. Qualitative and quantitative comparisons are made between computa-

S0024-9297(97)00964-9 CCC: $15.00
Published on Web 02/11/1998

tional results, light-scattering experiments, and morphological observations for the poly(methyl methacrylate (PMMA)/cyclohexanol system.[2] In this context, the validity of using current thermodynamic and kinetic theories to model structure growth in the vicinity of a glass transition is discussed.

Theory

According to standard Cahn−Hilliard theory, the diffusion equation describing structure formation during spinodal decomposition may be written as[17,18]

$$\frac{\partial \phi}{\partial t} = \nabla \cdot \left(M(\phi)\, \nabla \left(\frac{\partial f(\phi)}{\partial \phi} - 2\kappa \nabla^2 \phi \right) \right) \tag{1}$$

where $M(\phi)$ is the composition-dependent mobility, κ is the gradient energy parameter, f is the bulk free energy, and ϕ is the polymer volume fraction. A modified form of the Cahn−Hilliard equation, proposed by Cook,[19] has an additional stochastic term that accounts for thermal fluctuations. However, this term is only significant for shallow quenches in the transition region between NG and SD growth mechanisms.[4] Furthermore, it has been shown that the strength of the thermal noise has no effect on the late-stage growth exponent but only affects the approach to late stages.[20] Since our concern is primarily with the late-stage dynamics of fairly deep quenches into the spinodal region, thermal fluctuations are neglected. Moreover, experimental studies for polymer blends[21] and polymer solutions[2] near a glass transition have shown that structures grow by diffusive coarsening only. Therefore, hydrodynamic fluctuations are also neglected.

The free energy of the polymer−solvent system is modeled according to Flory−Huggins theory and can be written as

$$f = RT\left(\frac{\phi \ln \phi}{N} + (1-\phi)\ln(1-\phi) + \chi\phi(1-\phi) \right) \tag{2}$$

where f is now the free energy per mole of lattice sites, N is the degree of polymerization, and χ is the temperature-dependent interaction parameter. The gradient energy parameter is estimated from Debye's approximation[22] and is given by

$$\kappa = RT\chi R_G^{\,2}/6 \tag{3}$$

where R_G is the radius of gyration of the polymer which is typically evaluated by assuming unperturbed dimensions. Neglecting any temperature dependence of R_G, the temperature dependence of κ is very small over the regime of interest in this study and can be assumed constant.

The mobility is related to the solvent self-diffusion coefficient D_1 by

$$M = \frac{D_T}{\left(\frac{\partial^2 f}{\partial \phi^2} \right)} D_1 = \frac{\phi(1-\phi)}{\alpha(1-\phi)^2 + \phi(2\phi - 1)} D_1 \tag{4}$$

where D_T is a thermodynamic factor relating D_1 to the mutual diffusion coefficient. The form D_T should take has been debated in the literature.[23,24] Most recently, Vrentas and Vrentas[25] used a semiempirical approach to evaluate D_T which yields mutual diffusion coefficients that agree very well with experimental data. Approximating the y-parameter in eq 13 of ref 25 as N, the degree of polymerization, yields the relationship shown in eq 4. The parameter, α, is the ratio of D_1 to ND_2, in the dilute solution limit where D_2 is the polymer self-diffusivity which is estimated from the Kirkwood−Riseman theory.[26] Solvent self-diffusion coefficients for the PMMA/cyclohexanol system are estimated from the free-volume theory of Vrentas and Duda:[23,27]

$$D_1 = D_{01} \exp\left(\frac{-(\omega_1 V_1^* + \omega_2 V_2^*)}{V_{FH}/\gamma} \right) \tag{5}$$

where ω_i is the weight fraction of component i, V_i^* is the specific critical hole free volume of component i, γ is the average overlap factor for the mixture which is assumed to be unity, D_{01} is a preexponential factor assumed to be independent of temperature, and V_{FH} is the average specific hole free volume of the mixture given by

$$\frac{V_{FH}}{\gamma} = \omega_1 \frac{K_{11}}{\gamma_1}(K_{12} + T - T_{g1}) + \omega_2 \frac{V_{FH2}}{\gamma_2} \tag{6}$$

where K_{11} and K_{12} are free volume parameters, T_{g1} is the glass transition temperature of the pure solvent, and γ_1 and γ_2 are overlap factors for the pure component free volumes, which are assumed to be unity. The form of V_{FH2}, the specific hole free volume of the equilibrium liquid polymer, is a function of the state of the mixture, i.e., whether solution,[23] rubber,[28] or glass.[29] Since the temperatures in this study are below the glass transition of the pure polymer, the system is in the rubbery state ($T_{g,mix} < T < T_{g2}$) or glassy state ($T < T_{g,mix}$) and the following relations apply:

$$V_{FH2} = V_2^\circ(T_{g2})[f_{H2}^G - (\alpha_2 - \alpha_{c2})(T_{g2} - T)] \tag{7}$$

for the rubbery state and

$$V_{FH2} = V_2^\circ(T_{g2})[f_{H2}^G - \omega_1 A(\alpha_2 - \alpha_{2g} + \alpha_{c2g} - \alpha_{c2}) + (\alpha_{2g} - \alpha_{c2g})(T - T_{g2})] \tag{8}$$

for the glassy state, where V_2° is the specific volume of the equilibrium liquid polymer, α_i are thermal expansion coefficients, A is a parameter that measures the ability of the solvent to depress the glass transition of the system, $T_{g,mix}$, and f_{H2}^G is the fractional hole free volume of the polymer at its glass transition temperature, T_{g2}, which is related to the polymer free volume parameter, K_{22}. The various parameters for the PMMA/cyclohexanol system required by the Duda−Vrentas free volume equations are listed in Table 1 and the calculated mobilities are shown in Figure 1. The mobility function approaches zero in the pure component limits as a result of the composition-dependent prefactor in eq 4 and exhibits a relative maximum which is shifted to low polymer concentrations due to the presence of the glassy state at higher concentrations. More detailed discussions of the meaning of each parameter and the method of determination are given elsewhere.[27,28,30] The free volume parameters calculated for cyclohexanol differ slightly from those reported by Hong[31] but yield results that agree well with the phase separation dynamics observed in light-scattering experiments,[2] as will be shown.

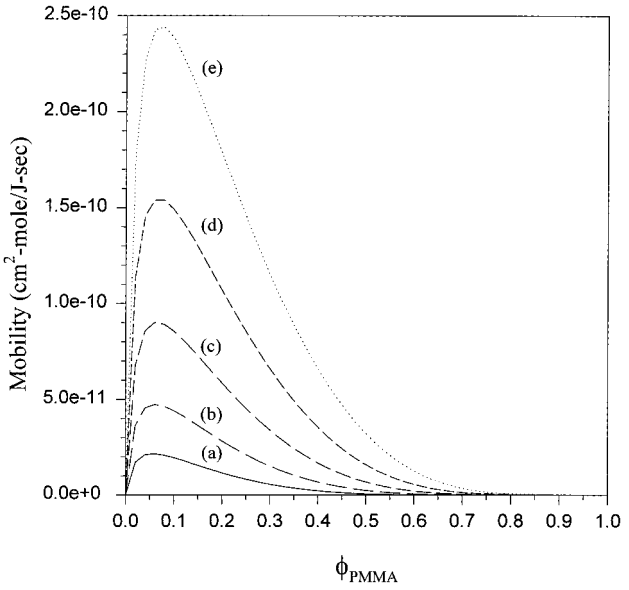

Figure 1. Mobility in the PMMA/cyclohexanol system as a function of polymer volume fraction for various temperatures (°C): (a) 20; (b) 30; (c) 40; (d) 50; (e) 60.

Table 1. Free-Volume Parameters for PMMA/ Cyclohexanol System

V_1^* (cm^3/g)	0.844
V_2^* (cm^3/g)	0.788
V_2° (cm^3/g)	0.8696
K_{11} (cm^3/g·K)	1.029×10^{-3}
K_{12} (cm^3/g K)	3.05×10^{-4}
K_{21} (K)	21.3
K_{22} (K)	80
T_{g1} (K)	217
T_{g2} (K)	378
ξ	0.586
D_{01} (cm^2/s)	1.26×10^{-3}
α	6.67×10^{-2}
α_2 (K^{-1})	5.8×10^{-4}
α_{2g} (K^{-1})	2.5×10^{-4}
α_{c2} (K^{-1})	2.0×10^{-4}
α_{c2g} (K^{-1})	0.866×10^{-4}
f_{H2}^G	0.0464
A (K)	250

Numerical Method

Scaling. The Cahn−Hilliard equation can be scaled using the following dimensionless quantities:

$$x^* = x/L \tag{9}$$

$$\tau = (2\kappa M_0/L^4)t \tag{10}$$

$$F = f/RT \tag{11}$$

where x^* is a dimensionless length, τ is a dimensionless time, M_0 is a scaling constant having units of mobility, and L is the scaling length given by

$$L = a(2\kappa/RT)^{1/2} \tag{12}$$

where a is an adjustable parameter between 0.5 and 2 used to ensure the appropriate size scales are being investigated for each simulation. Using eqs 9−11, eq 1 becomes

$$\frac{\partial\phi}{\partial\tau} = \nabla^*\cdot\left(M^*(\phi)\,\nabla^*\left(a^2\,\frac{\partial F(\phi)}{\partial\phi} - \nabla^{*2}\phi\right)\right) \tag{13}$$

where M^* and ∇^* are also dimensionless quantities given by M/M_0 and $L\nabla$, respectively.

Discretization. Equation 13 is discretized using a standard explicit scheme:[32]

$$\frac{\phi_{i,j}^{n+1} - \phi_{i,j}^{n}}{\Delta\tau} = \frac{J_{i+1/2,j} - J_{i-1/2,j} + J_{i,j+1/2} - J_{i,j-1/2}}{\Delta x^*} \tag{14}$$

where $J_{i+1/2,j}$ is the total flux at point $(i + {}^1/_2, j)$ and is given by

$$J_{i+1/2,j} = M_{i+1/2,j}^*\left(\frac{\mathrm{d}F/\mathrm{d}\phi_{i+1,j} - \mathrm{d}F/\mathrm{d}\phi_{i,j}}{\Delta x^*} - \frac{\nabla^{*2}\phi_{i+1,j} - \nabla^{*2}\phi_{i,j}}{\Delta x^*}\right) \tag{15}$$

where

$$\nabla^{*2}\phi_{i,j} = \frac{\phi_{i+1,j} + \phi_{i,j+1} - 4\phi_{i,j} + \phi_{i-1,j} + \phi_{i,j-1}}{\Delta x^*} \tag{16}$$

This scheme is used to numerically integrate eq 13 on a 64 × 64 or 128 × 128 grid with the assumption of periodic boundary conditions. Care was taken in the choice of the mesh size, Δx^*, to avoid possible discretization artifacts such as mesh-size dependence[20] and artificial pinning effects.[10] It was determined that values for Δx^* between 0.7 and 1.0 were adequate for computations.

Data Analysis. The time evolution of the two-phase structure is quantified using the structure factor, $S(\mathbf{k},t)$, which is simply the square of the magnitude of the Fourier transform, $A(\mathbf{k},t)$, of the concentration fluctuations in the system.

$$S(\mathbf{k},t) = |A(\mathbf{k},t)|^2 = \left|\sum_{m=0}^{N-1}\sum_{n=0}^{N-1}(\phi_{m,n} - \phi_0)\exp\left(\frac{2\pi i}{N}(mk_x + nk_y)\right)\right|^2 \tag{17}$$

where $\phi_{m,n}$ is the volume fraction of polymer at node (m, n), ϕ_0 is the mean volume fraction, and $\mathbf{k}$ is the 2D position vector, (k_x, k_y), in Fourier space. The structure factor offers direct comparison with light-scattering experiments since it is proportional to the scattering intensity.[33] A similarly useful quantity is the pair correlation function, $G(\mathbf{r},t)$, which is the Fourier transform of $S(\mathbf{k},t)$:

$$G(\mathbf{r},t) = \sum_k \exp(i\mathbf{k}\cdot\mathbf{r})S(\mathbf{k},t) \tag{18}$$

Since the phase separation is isotropic, analysis can be improved by using circularly averaged quantities, $S(k,t)$ and $G(r,t)$ where k and r are the distances from the center of the Fourier space plane and real space plane, respectively.[3,34] The position of the maximum of the structure factor, k_m, and the first zero of the pair correlation function, r_1, are used as measures of the domain size, since both are proportional to the position of the light-scattering intensity maximum. Owing to discretization, k_m is difficult to determine accurately, particularly at larger times where the spinodal ring is collapsing. As a result, a better measure of domain size

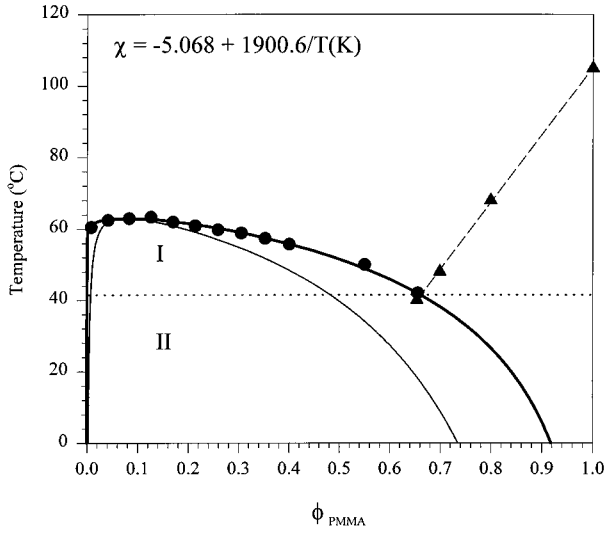

Figure 2. Phase diagram for the PMMA/cyclohexanol system: (●) data of Graham et al.;[2] (▲) data of Vanderweerdt et al.;[36] (thick line) calculated binodal; (thin line) calculated spinodal; (dashed line) glass transition curve. Regions I and II correspond respectively to phase separation above and below the glass transition.

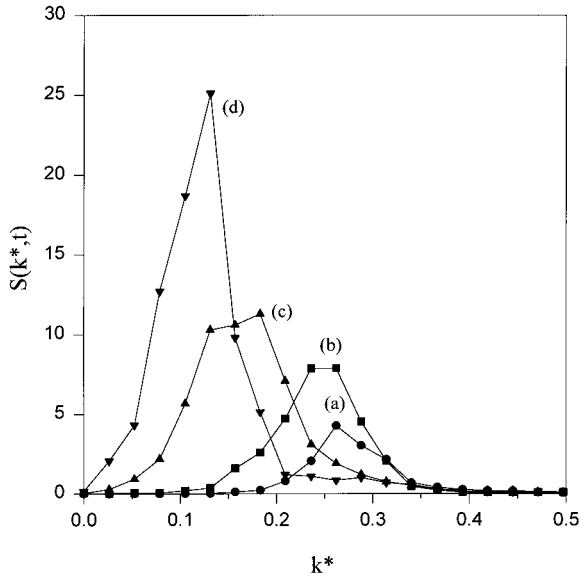

Figure 3. Structure factor as a function of k^*, the dimensionless radial position in Fourier space, for a quench to 50 °C for a 35 wt % PMMA/cyclohexanol solution. Quench times $\tau^* = a^4\tau$: (a) 1700; (b) 3000; (c) 12 200; (d) 30 400.

in discrete Fourier space is the first moment of the structure factor, k_1, given by

$$k_1 = \frac{\sum_k kS(k,t)}{\sum_k S(k,t)} \tag{19}$$

This quantity can be determined more accurately than k_m since it is calculated from data over the entire range of wave vectors, and it has been shown to scale in the same manner with time as k_m.[11]

Results and Discussion

To check the validity of the numerical scheme, simulations were performed on a number of systems previously considered in the literature. For example, excellent agreement was obtained with the results of Copetti and Elliott[35] for a system with constant mobility and the predictions of Rousar and Nauman[32] for a symmetric polymer blend.

The phase diagram for the PMMA/cyclohexanol system considered for the present simulations is shown in Figure 2. The temperature dependence of χ was determined from Flory−Huggins theory by fitting the calculated binodal to the cloud-point data of Graham et al.[2] A composition dependence was also considered; however, the best fit was obtained by assuming χ to be a function of temperature only. A degree of polymerization of 150 was used in these calculations, which is consistent with the molecular weight of PMMA used in cloud-point measurements and light-scattering observations.[2] The glass transition line is a linear fit of the data of Venderweerdt et al.[36] The theory of Kelley−Bueche[37] yields similar results over the temperature regime explored in this study. Light-scattering experiments[2] have shown that, for quenches to region I of the phase diagram, i.e., above the glass transition region, the resultant two-phase structure grows as $t^{1/3}$, as predicted by late-stage theories for diffusion-limited coarsening.[38,39] However, further quenching into region II, below the glass transition, results in cessation of structure growth and an apparent freezing of the two-phase morphology.[2]

To model these effects, quenches of an initially homogeneous 35 wt % PMMA/cyclohexanol solution to regions I and II of the phase diagram were simulated. The results presented herein represent runs from a single initial configuration. Multiple runs were conducted only to check for consistency and, therefore, no averaging of results over several initial configurations was performed. Figure 3 shows the evolution of the circularly averaged structure factor following a quench to 50 °C. A discernible maximum forms during the early stages of structure formation which increases in intensity and shifts to lower k^* values with time, indicating an increase in the size of the phase-separated domains. A power law fit shows that the position of, k_1^*, scales as $t^{-0.35}$, in good agreement with light-scattering observations.[2] The evolution of the pair correlation function is shown in Figure 4. The shift of the first zero, r_1^*, to higher values is also indicative of domain coarsening. For a direct comparison to the experimentally observed scattering maximum, the evolution of the inverse quantity, $2\pi/r_1^*$, is shown in Figure 5 for quenches above the glass transition region. The slope of the least-squares fit shows that, at 50 °C, $2\pi/r_1^*$ decays as $t^{-0.37}$, also consistent with experiment. The slight difference in the exponent reflects the way in which the dominant size scale is estimated. The corresponding two-phase morphologies at points a−c in Figure 5 are shown in Figure 6a−c. The morphology during the early stage (not shown) is bicontinuous. However, the polymer-lean phase rapidly breaks apart, resulting in a droplet type morphology composed of solvent-rich pores surrounded by a polymer-rich matrix. This evolution is consistent for an off-critical quench into the spinodal region, whereby the initial structure undergoes a percolation-to-cluster transition.[40] This behavior has also been observed in computational[4,16,34] and experimental[5] studies.

The effect of a second quench to 25 °C on the coarsening of the morphology is also shown in Figure

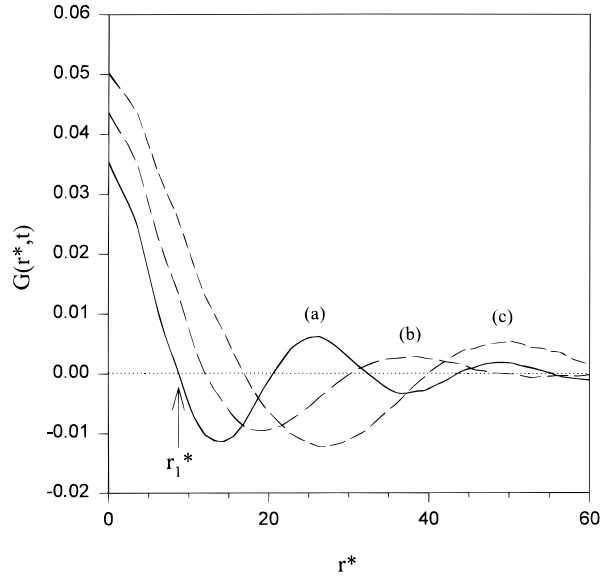

Figure 4. Pair correlation function for a quench to 50 °C for a 35 wt % PMMA/cyclohexanol solution. Quench times $\tau^* = a^4\tau$: (a) 3000; (b) 12 200; (c) 30 400.

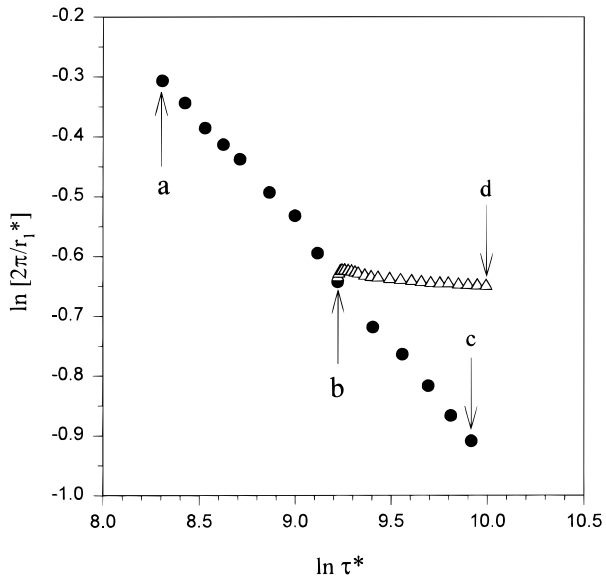

Figure 5. Evolution of structure size for (●) quench to 50 °C and (△) a second quench to 25 °C during late-stage coarsening. Points a−d correspond to the morphologies shown in Figure 6.

5d. These simulations were conducted using mobilities in the glassy state calculated from eqs 4 and 5 which yield values typically 1−3 orders of magnitude smaller than the solution-state mobilities. Results show that, because the glassy-state mobilities are still finite, coarsening is not completely arrested. Similar behavior was also observed by Sappelt and Jackle[13,14] in their simulations of phase separation in a glassy mixture. However, as shown in Figure 5d, over the time scale of the simulations, the average pore size, as measured by k_m, remains unchanged. Moreover, when extrapolated to experimental length scales, these results show that structure growth is effectively arrested on experimental time scales, in excellent agreement with the data of Graham et al.[2,41] Although the initial droplet morphology is still obvious, a secondary, solvent-rich droplet phase also forms within the polymer-rich matrix, as shown in Figure 6d. In addition, as shown in Figure 7, we find that the secondary phase has only a small effect on the calculated structure factor at higher k^*. Micrographs of morphology,[42] prepared by quenching below the glass transition, show strong evidence of secondary pores within the polymer-rich matrix. This secondary structure is a result of the polymer-rich phase formed at 50 °C being thermodynamically unstable at 25 °C. Figure 2 clearly shows that the equilibrium composition of the polymer-rich phase at 50 °C lies within the spinodal region at 25 °C. Therefore, spinodal decomposition proceeds in the polymer-rich matrix until the glass composition is reached, at which point further growth proceeds slowly, so that on experimental time scales growth effectively ceases.

The pore growth rate during the late stages for a given quench is determined by fitting the time evolution data for r_1^* to the growth law expression[43]

$$R^3 = R_0^3 + K(t - t_0) \tag{20}$$

where K is the pore growth rate constant, R is the size of the droplet phase at time, t, and R_0 is the size at t_0, the time required for the early stage of spinodal decomposition. K was determined from simulations for several quench temperatures, and the resulting extrapolated pore growth curves are shown in Figure 8. A similar analysis can be performed on light-scattering data for the PMMA/cyclohexanol system,[2] where R is related to the wavenumber of the scattering intensity maximum, q_m, by

$$R = 2\pi/q_m \tag{21}$$

However, in the experimental case, t_0 in eq 20 represents the time required for thermal equilibration of the quenched solution, which can be several seconds in duration. The pore growth curves for these data are given in Figure 9. Immediately apparent from Figures 8 and 9 is the close correspondence between calculated and experimental growth rates. This is, in some sense, surprising, considering that our Cahn−Hilliard simulations contain no free parameters. Moreover, the calculated and experimental curves both exhibit a decrease in the pore growth rate with decreasing temperature or increasing quench depth, ΔT. However, over the complete range of temperatures explored in simulations, the pore growth rate exhibits a relative maximum, as shown in Figure 10. This suggests that there is a complex interplay between the transport kinetics and the thermodynamic driving force for phase separation which determine the temperature dependence of the growth rate.

The separate effects of the transport and thermodynamics on the growth rate were elucidated by performing two series of simulations: one with a temperature-independent mobility function and the other with a temperature-independent free energy (constant χ). The results are shown in Figure 10. When the thermodynamics dominates, the pore growth rate shows an increase with increasing quench depth. This corresponds to a system undergoing phase separation far removed from a glass transition and, indeed, such a trend has been observed in light-scattering data on a quenched polyethylene copolymer/anisole system[44] and in microscopy for several other solution systems.[41,45,46] However, when transport effects dominate, the growth rate is seen to decrease with increasing quench depth. This behavior is observed in the PMMA/cyclohexanol

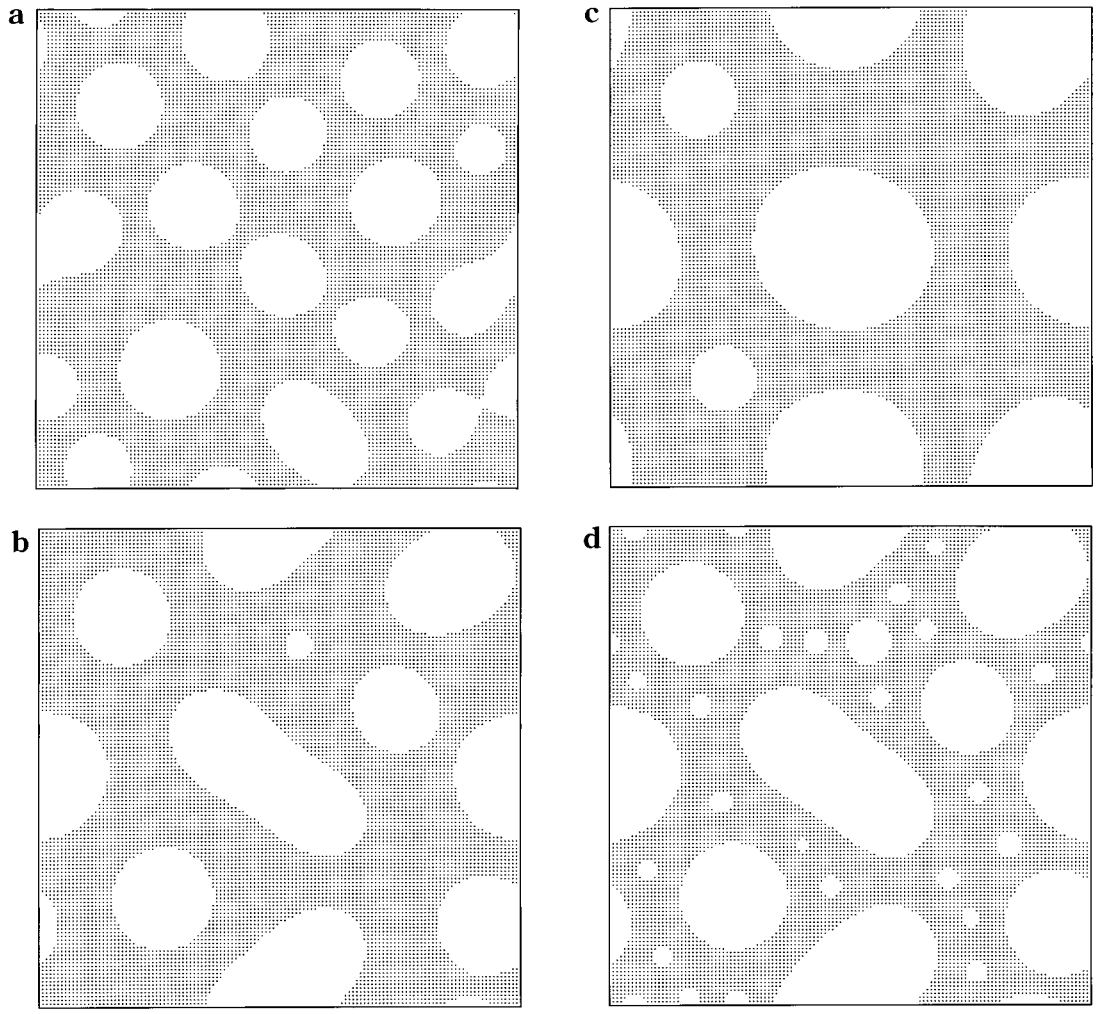

Figure 6. Evolution of morphology for a quench to 50 °C at times corresponding to points a−d in Figure 5: (a) $\tau^* = 4000$; (b) $\tau^* = 10\,000$; (c) $\tau^* = 20\,000$; (d) $\tau^* = 22\,000$ after a second quench to 25 °C at $\tau^* = 10\,000$.

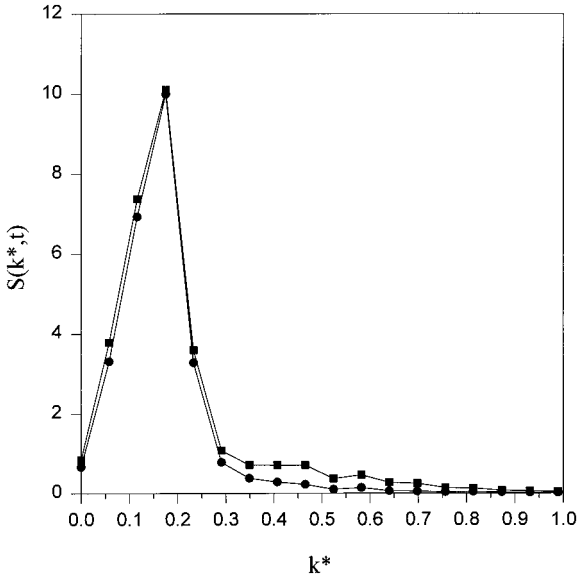

Figure 7. Structure factor at (●) $\tau^* = 10\,000$, just before quench to 25 °C and (■) $\tau^* = 22\,000$, following quench to 25 °C.

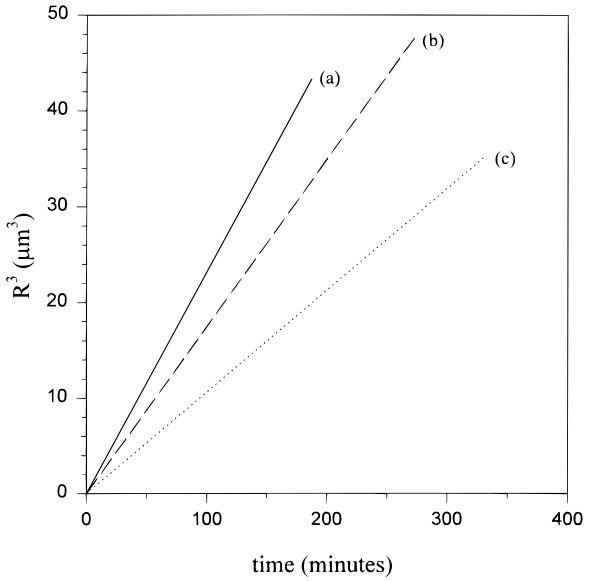

Figure 8. Extrapolated late-stage growth curves from simulated quenches. $\Delta T = T_{quench} - T_{spinodal}$: (a) $\Delta T = 11$ °C; (b) $\Delta T = 14$ °C; (c) $\Delta T = 17$ °C. Calculated growth rates in $\mu m^3/s$: (a) 0.0039; (b) 0.0029; (c) 0.0018.

system over the experimental regime studied and is a result of phase separation dynamics occurring near a glass transition.[2] Therefore, the maximum in the pore growth rate predicted for the PMMA/cyclohexanol system is a result of a crossover from a regime where thermodynamics is rate-controlling to one where transport effects dominate.

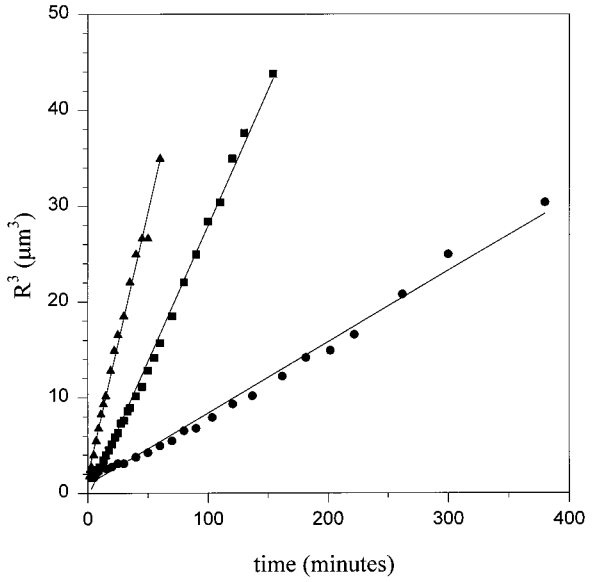

Figure 9. Late-stage growth curves from light-scattering experiments:[2] quench to (▲) 54, (■) 50, and (●) 47 °C. Fitted growth rates in $\mu m^3/s$: 0.0092, 0.0048, 0.0012, respectively.

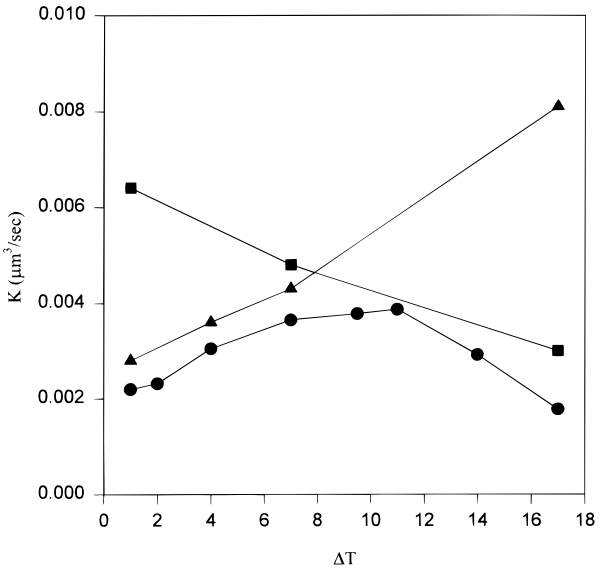

Figure 10. Calculated pore growth rates (●) for PMMA/cyclohexanol system; (▲) using a temperature-independent mobility function, $M/M_0 = \phi(1 - \phi)$ [thermodynamics dominate]; (■) using a temperature-independent free energy function with $\chi = 0.8686$ [kinetics dominate]. Constant M and constant χ curves are shifted arbitrarily along the K-axis to better show trends with quench depth.

Another important result from these simulations, shown in Figure 11, is the extreme shortness of the time periods for early-stage phase separation. These ranged from 5 to 150 μs over the regime studied and scaled as $\Delta T^{-1.5}$. This clearly suggests the unlikelihood of experimentally observing early-stage structure growth in most polymer solutions. Moreover, since experimental time scales for temperature transients during the quench period are typically much longer (i.e., on the order of seconds to minutes), care is needed in interpreting scattering behaviors. For example, light-scattering data for our PMMA/cyclohexanol system[2] exhibit an apparent early-stage regime on log−log coordinates ranging from several seconds to several minutes in length and are suggestive of constant size of the spinodal structure. We believe this behavior is simply

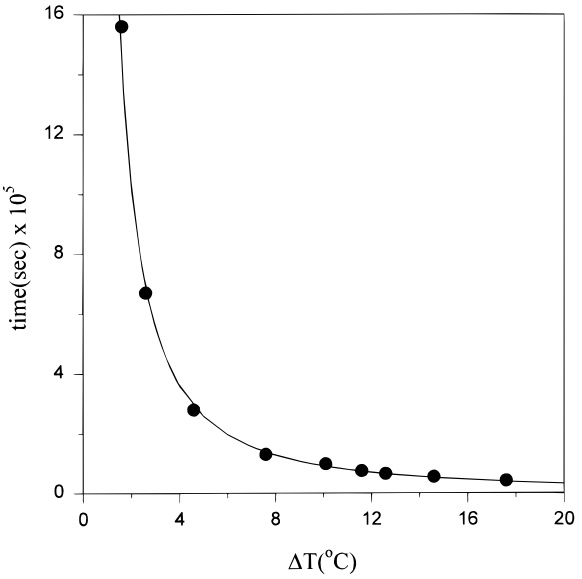

Figure 11. Time required for completion of early-stage coarsening as a function of quench depth, $\Delta T = T_{quench} - T_{spinodal}$.

the result of late-stage growth of structures which formed during the transient quench period prior to temperature equilibration.[40] Clearly, once the final spinodal temperature is reached, the dynamics one sees are those of late stage. As noted by Crist,[43] the effect of the initial structure, R_0, on the growth dynamics can be exaggerated when plotted on a log−log scale, giving the appearance of early-stage or pinned behavior. The fit of the light-scattering data to eq 20, as shown in Figure 9, demonstrates that $t^{1/3}$ scaling is followed over the entire experimental time regime.

Conclusions

In this work, simulations of phase separation in the PMMA/cyclohexanol system based on the Cahn−Hilliard model have been shown to yield excellent agreement with experimental results. Current theories used to estimate thermodynamic and kinetic parameters for polymer solutions are adequate for qualitative and quantitative prediction of the phase separation dynamics near a glass transition, as well as the resultant morphology. Quenching a phase-separated solution below the glass transition boundary effectively freezes the preexisting morphology. However, prior to attaining the glass transition composition, a secondary droplet structure forms as a result of the polymer-rich matrix undergoing a second spinodal decomposition process. Strong morphological evidence exists for such behavior. However, since the secondary structure has little impact on the calculated structure factor, this phenomenon probably cannot be confirmed through light-scattering observations. Care must be taken in interpreting light-scattering results for polymer solutions which appear to exhibit early-stage behavior. These data are not due to early-stage spinodal decomposition but are a result of late-stage growth in a transient temperature field. This is certainly the case for the PMMA/cyclohexanol system, as calculations show that the early stages of structure formation occur too rapidly to be observed experimentally. Analysis of our light-scattering measurements[2] using eq 20 clearly shows that the data follow late-stage dynamics from the onset of pattern formation.

Acknowledgment. This work has been supported under a grant from the National Science Foundation (Grant CTS 94-21580).

References and Notes

(1) Lal, J.; Bansil, R. *Macromolecules* **1991**, *24*, 290.
(2) Graham, P. D.; Pervan, A. J.; McHugh, A. J. *Macromolecules* **1997**, *30*, 1651.
(3) Gunton, J. D.; San Miguel, M.; Sahni, P. S. The Dynamics of First-Order Transitions. In *Phase Transitions and Critical Phenomena*; Domb, C., Lebowitz, J. L., Eds.; Academic Press: New York, 1983; Vol. 8, p 267.
(4) Chakrabarti, A. *Phys. Rev. B* **1992**, *45*, 9620.
(5) Tanaka, H.; Yokokawa, T.; Abe, H.; Takafumi, H.; Nishi, T. *Phys. Rev. Lett.* **1990**, *65*, 3136.
(6) Brown, G.; Chakrabarti, A. *J. Chem. Phys.* **1993**, *98*, 2451; *Phys Rev. E* **1993**, *48*, 3705.
(7) Zhang, H.; Zhang, J.; Yang, Y. *Macromol. Theory Simul.* **1995**, *4*, 1001.
(8) Vasishtha, N.; Nauman, E. B. *Chem. Eng. Commun.* **1994**, *129*, 29.
(9) Matsuoka, T.; Yamamoto, S. *J. Appl. Polym. Sci.* **1995**, *57*, 353.
(10) Castellano, C.; Glotzer, S. C. *J. Chem. Phys.* **1995**, *103*, 9363.
(11) Glotzer, S. C.; Gyure, M. F.; Sciortino, F.; Coniglio, A.; Stanley, H. E. *Phys. Rev. E* **1994**, *49*, 247 and references therein.
(12) Sciortino, F.; Bansil, R.; Stanley, H. E. *Phys. Rev. E* **1993**, *47*, 4615.
(13) Sappelt, D.; Jackle, J. *Europhys. Lett.* **1997**, *37*, 13.
(14) Sappelt, D.; Jackle, J. *Physica A* **1997**, *240*, 453.
(15) Caneba, G. T.; Soong, D. S. *Macromolecules* **1985**, *18*, 2545. Chen, Y.; Solc, K.; Caneba, G. T. *Polym. Eng. Sci.* **1993**, *33*, 1033.
(16) Chan, P. K.; Rey, A. D. *Macromol. Theory Simul.* **1995**, *4*, 873.
(17) Cahn, J. W.; Hilliard, J. E. *J. Chem. Phys.* **1958**, *28*, 258.
(18) Novick-Cohen, A.; Segel, L. A. *Phys. D* **1984**, *10*, 277.
(19) Cook, H. E. *Acta Metall.* **1970**, *18*, 297.
(20) Rogers, T. M.; Elder, K. R.; Desai, R. C. *Phys. Rev. B* **1988**, *37*, 9638.
(21) Kuwahara, N.; Sato, H.; Kubota, K; *Phys. Rev. E* **1993**, *47*, 1132.
(22) Debye, P. *J. Chem. Phys.* **1959**, *34*, 680.
(23) Vrentas, J. S.; Duda, J. L. *J. Polym. Sci.* **1977** *15*, 417.
(24) Duda, J. L.; Ni, Y. C.; Vrentas, J. S. *Macromolecules* **1979**, *12*, 459.
(25) Vrentas, J. S.; Vrentas, C. M. *Macromolecules* **1993**, *26*, 6129.
(26) Vrentas, J. S.; Duda, J. L. *J. Appl. Polym. Sci.* **1976**, *20*, 1125.
(27) Vrentas, J. S.; Duda, J. L. *J. Polym. Sci.* **1977**, *15*, 403.
(28) Vrentas, J. S.; Vrentas, C. M. *Macromolecules* **1994**, *27*, 4684.
(29) Vrentas, J. S.; Vrentas, C. M. *Macromolecules* **1994**, *27*, 5570.
(30) Zielinski, J. M.; Duda, J. L. *AIChE J.* **1992**, *38*, 405.
(31) Hong, S. *Ind. Eng. Chem. Res.* **1995**, *34*, 2536.
(32) Rousar, I.; Nauman, E. B. *Chem. Eng. Commun.* **1991**, *105*, 77.
(33) Tanaka, H.; Hayashi, T.; Nishi, T. *J. Appl. Phys.* **1986**, *59*, 3627.
(34) Chan, P. K.; Rey, A. D. *Macromol. Theory Simul.* **1995**, *4*, 873.
(35) Copetti, M. I. M.; Elliott, C. M. *Mater. Sci. Technol.* **1990**, *28*, 273.
(36) Vanderweerdt, P.; Berghmans, H.; Tervoort, Y. *Macromolecules* **1991**, *24*, 3547.
(37) Kelley, F. N.; Bueche, F. *J. Polym. Sci.* **1961**, *50*, 549.
(38) Binder, K.; Stauffer, D. *Phys. Rev. Lett.* **1974**, *33*, 1006.
(39) Lifshitz, I. M.; Slyozov, V. V. *J. Phys. Chem. Solids* **1961**, *19*, 35.
(40) Binder, K. *Solid State Commun.* **1980**, *34*, 191.
(41) Graham, P. D. Master's Thesis, University of Illinois, Urbana, IL, 1996.
(42) Song, S.-W.; Torkleson, J. M. *J. Membr. Sci.* **1995**, *98*, 209.
(43) Crist, B. *Macromolecules* **1996**, *29*, 7276.
(44) Graham, P. D.; McHugh, A. J. *Macromolecules*, in press.
(45) Song, S.-W.; Torkleson, J. M. *Macromolecules* **1994**, *27*, 6389.
(46) McGuire, K. S.; Laxminarayan, A.; Lloyd, D. R. *Polymer* **1995**, *36*, 4951.

MA970964J